In situ estimation of acoustic impedance on the surfaces of realistic interiors: an inverse approach

Gabriel Pablo Nava*, Yoichi Sato, Shinichi Sakamoto
Institute of Industrial Science, University of Tokyo,
Komaba 4–6–1, Meguro-ku, Tokyo, 153-8505, JAPAN.

Yosuke Yasuda
Graduate School of Frontier Sciences, University of Tokyo,
Kashiwanoha 5–1–5, Kashiwa-shi, Chiba, 277-8563, JAPAN.

November 30, 2007

Abstract

In situ measurement of acoustic impedance is traditionally performed using pairs of microphones located close to the test surface. However, this method becomes troublesome if inaccessible complex-shaped surfaces, such as those in a real room, are considered. To overcome this problem a method to estimate the normal acoustic impedance on the interior surfaces of a room is proposed. As input data, the algorithm takes: 1) the 3D shape of the room, 2) the strength of the sound source, and 3) a set of sound pressures measured at random locations in the interior sound field. The estimation of the acoustic impedance at each surface is achieved via the solution of an inverse problem which arises from the boundary element method applied to the discretized interior boundaries of the room. Unfortunately, the solutions of this kind of problems are known to be unstable and sensitive to noise due a rank-deficient linear system. Dealing with such a system is avoided in the proposed method by formulating an iterative optimization approach which is shown to be more robust to noise. Previous work has reported examples with numerical simulations. This paper goes further and presents results obtained with real data from experiments.

KEYWORDS: in situ measurements, inverse boundary element method, iterative optimization

*Corresponding author. E-mail: pablo@iis.u-tokyo.ac.jp

1 Introduction

Numerical algorithms for the previsualization of sound fields have become advanced and successfully used in a wide range of applications. However, in order to achieve accurate predictions of sound, most of these simulations tools (e.g. BEM and FEM) require the assessment of acoustic parameters that are directly related to the acoustic properties of the materials, and therefore, these parameters have to be experimentally measured.

Although laboratory methods used to measure acoustic properties of the materials provide important information, they usually rely on assumptions of ideal conditions that are not frequently met in practice. On the other hand, traditional in situ measurement methods (e.g. [1, 2, 3, 4]) suffer basically from one or all of the following geometrical constraints: 1) the test material should be flat and large; 2) the measurements must be isolated from sound reflections different from those coming from the test surface, this is, the measurements should be performed in a large space (preferably open) or in an anechoic room; 3) the measuring microphones (usually a pair) should be placed either, right close to the test surface, or at an specific distance from the surface. A recent method tries to alleviate some of these by employing a particle velocity and a sound pressure sensors integrated in a single package known as "microflown" [5]. Placing the microflown close to the test material, what is actually being measured is the acoustic impedance of the incident wave at the vicinity of the surface. Another effort to developed a universally applicable in situ measurement method was reported by Takahashi *et. al.* [6]. The principle of this method is based on averaging, over time and angle of incidence, the measured sound coming from the ambient noise. Hence, this approach assumes random incidence of plane waves in a uniformly diffused field. Condition that in practical situations is hardly found.

Compared with traditional methods, in this paper, the estimation of normal-incidence acoustic impedance is formulated as an inverse boundary problem, which allows us to overcome most of the geometrical constraints discussed before. Similar inverse acoustic problems have been studied in previous work for the identification of sound sources on the surface of vibrating bodies (the near-field acoustic holography is the most representative approach in this field, e.g. [7]), however, a few work has been done for the estimation of acoustic impedance in this context. One of the first reported inverse approaches to estimate the surface acoustic impedance was made by Dutilleux *et. al.* [8], who used a framework based on the finite element method (FEM) combined with evolution strategies (ES) to perform numerical simulations with simple-shaped interiors. Although FEM is a widely used numerical tool, let us note that the boundary element method (BEM) is a more efficient framework to model the interaction between an interior sound field and its boundaries. Moreover, because of the discrete linear equations derived with the BEM, it is possible to formulate an iterative optimization algorithm that yields the estimation of the acoustic impedances of not only one but all the surfaces of an interior space.

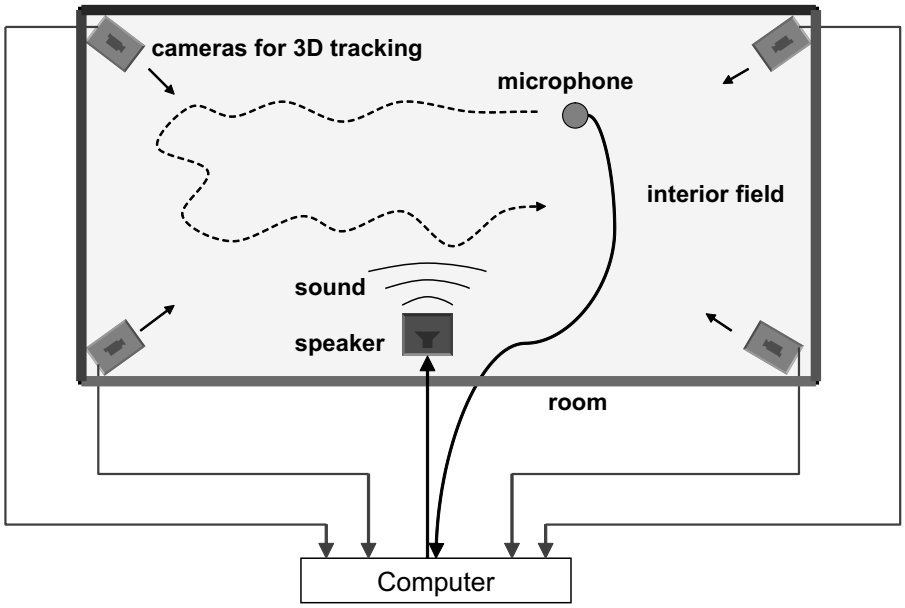

Figure 1: Setup of the inverse estimation of the acoustic impedance on the interior surfaces of a room.

2 Description of the framework

Let us suppose that the acoustic impedance of the interior surfaces of the room depicted in Figure 1 are to be estimated using the set up illustrated. The measurement procedure is as follows: 1) specify the sound frequency at which the acoustic impedance is desired, 2) emit a tone of the selected frequency through the speaker, 3) start the measurement process, 4) move the microphone freely along the room until the necessary number of measurements of sound pressure have been acquired by the system, 5) stop the measurement process and start the data processing. To estimate the acoustic impedance of all the surfaces within the room, the algorithm takes as input: 1) the geometric model of the room, 2) the position and the vibration strength of the speaker, and 3) a set of sound measurements taken at M random points in the interior field. With this information, the derivation of the algorithm is as follows below.

The sound pressure p_f at any point in the steady-state interior field of Figure 1 is related to the sound pressure p_S and particle velocity v_S on the surfaces by the Helmholtz-Kirchhoff equation

$$\oint_S \left(p_S \frac{\partial \mathrm{G}(r)}{\partial \mathbf{n}} + j\omega\rho \mathrm{G}(r)\ v_S \right) dS + p_f = 0\ , \tag{1}$$

where $\mathrm{G}(r)$ denotes the three dimensional Green's function $\mathrm{G} = e^{-jkr}/4\pi r$, with r the euclidian distance between a point on a surface and a field point, k the wave number, ρ the density of the field, and $j = \sqrt{-1}$. Note that the sought impedance values at the surfaces are defined by the relation $Z_S = p_S/v_S$.

When the 3D model of the room is discretized into N constant elements and M field points are considered, it can be shown that the BEM formulation of the interior field yields the following matrix equations:

$$\mathbf{A}_S\ \mathbf{p}_S - \mathbf{B}_S\ \mathbf{v}_S \ = \ 0\ , \tag{2}$$

$$\mathbf{A}_f\ \mathbf{p}_S - \mathbf{B}_f\ \mathbf{v}_S \ = \ -\ \mathbf{p}_f\ . \tag{3}$$

If constant elements of the 3D mesh are considered, the entries of the matrices $\mathbf{A}$'s and $\mathbf{B}$'s are computed as

$$a_{i,k} \ = \ \oint_{S_k} \frac{\partial \mathrm{G}(r)}{\partial \mathbf{n}}\ \mathrm{ds} \quad , \qquad b_{i,k} \ = \ -\ j\omega\rho \oint_{S_k} \mathrm{G}(r)\ \mathrm{ds}\ , \tag{4}$$

with $i = 1, 2, \ldots, M$ and $k = 1, 2, \ldots, N$. Thus, the matrices $\mathbf{A}_S$ and $\mathbf{B}_S$ represent the influence coefficients between two different points on the surface. Similarly, $\mathbf{A}_f$ and $\mathbf{B}_f$ contain the influences between a point on the surface and a point in the field. Furthermore, since the vibration strength of the sound source is assumed to be known, equation (3) can be rewritten as

$$\mathbf{A}_f\mathbf{p}_S - \widetilde{\mathbf{B}}_f\widetilde{\mathbf{v}}_S = \widehat{\mathbf{B}}_f\widehat{\mathbf{v}}_S - \mathbf{p}_f\ , \tag{5}$$

denoting by $\widehat{\mathbf{v}}_S$ and $\widehat{\mathbf{B}}_f$ the known particle velocities and their corresponding influence coefficients, and by $\widetilde{\mathbf{v}}_S$ the unknowns with their corresponding known influence coefficients $\widetilde{\mathbf{B}}_f$.

In the 3D model, the interior surfaces have been segmented by homogeneity giving a total of n different surfaces such $\{S_i \mid S = S_1 \cup S_2 \ldots S_n,\ \forall\ i = 1, 2, \ldots, n\}$. If it is further assumed that the surfaces are basically locally reactive, the following approximation can be considered:

$$\frac{p_{S_i,1}}{v_{S_i,1}} \approx \frac{p_{S_i,2}}{v_{S_i,2}} \approx ... \approx \frac{p_{S_i,m_i}}{v_{S_i,m_i}}\ , \tag{6}$$

or

$$z_{S_i,1} \approx z_{S_i,2} \approx \ldots \approx z_{S_i,m_i} = Z_i\ , \tag{7}$$

here, m_i indicates the number of discrete nodes that belong to the i-th surface.

Substituting the surface sound pressures $\mathbf{p}_S$ of equation (5) by their equivalent impedance effect, and grouping the nodal impedances according to equation (7), the following linear system is derived:

$$\langle \mathbf{A}_f \cdot \tilde{\mathbf{v}}_S \rangle\ \mathbf{z} - \tilde{\mathbf{B}}_f\tilde{\mathbf{v}}_S = \hat{\mathbf{p}}_f\ , \tag{8}$$

where

$$\langle \mathbf{A}_f \cdot \tilde{\mathbf{v}}_S \rangle = \begin{pmatrix} \sum_{k=1}^{m_1} a_{f,(1,k)}\ \tilde{v}_{S,k} & \sum_{k=m_1+1}^{m_2} a_{f,(1,k)}\ \tilde{v}_{S,k} & \cdots & \sum_{k=m_{n-1}+1}^{m_n} a_{f,(1,k)}\ \tilde{v}_{S,k} \\ \vdots & \vdots & \cdots & \vdots \\ \vdots & \vdots & \cdots & \vdots \\ \sum_{k=1}^{m_1} a_{f,(M,k)}\ \tilde{v}_{S,k} & \sum_{k=m_1+1}^{m_2} a_{f,(M,k)}\ \tilde{v}_{S,k} & \cdots & \sum_{k=m_{n-1}+1}^{m_n} a_{f,(M,k)}\ \tilde{v}_{S,k} \end{pmatrix} ,$$

$$\mathbf{z} = \{Z_1, Z_2, \ldots, Z_n\} ,$$

$$\hat{\mathbf{p}}_f = \hat{\mathbf{B}}_f \hat{\mathbf{v}}_S - \mathbf{p}_f .$$

The parameters $\tilde{\mathbf{v}}_S$ and $\mathbf{z}$ in equation (8) are both unknowns, thus, in order to estimate the desired impedance values, equation (8) is iteratively solved for $\mathbf{z}$ according to the steps of Algorithm 1.

To start the iterative process, an initial guess is proposed $\mathbf{z}^{(0)} = \{Z_1^{(0)}, Z_2^{(0)}, \ldots, Z_n^{(0)}\}$, and assuming that the sought impedances lay within some maximum and minimum values, bounds can be specified as $\mathrm{Z_{min}} \leq \mathbf{z} \leq \mathrm{Z_{max}}$ to the solution space.

The entries of the matrices $\mathbf{C}$'s in equations (9) and (11) are computed as $c_{i,k} = z_{S,k} \cdot a_{i,k}$.

At each iteration, a set of predicted sound pressures $\mathbf{p}_g$ computed at the same points of the measured field pressures is compared with the actual measurements $\mathbf{p}_f$ according to equation (12), until the error is less than the specified threshold α. The selection of this parameter is crucial since it determines the stopping criterion. In practice, if too small values are assigned to α, the condition (12) is not achieved and the process has to be stopped before the solutions fit the noise level. Finally, at step 3 of Algorithm 1, the update of $z^{(\ell+1)}$ involves the solution of equation (10) which is solved by a nonlinear optimization process using Sequential Quadratic Programing (SQP). The implemented routine of the latter is available as a function in the commercial software Matlab.

3 Experimental setup

In order to verify the algorithm introduced in the previous section, preliminary validation experiments were performed in a controlled environment in the interior of a reverberation chamber made of 3 mm-thick acrylic with dimensions as shown in Figure 2. The actual experimental chamber can be seen in Figure 3a.

The experiment consists on the estimation of the normal acoustic impedance of four surfaces defined by homogeneity materials placed in the interior of the chamber.

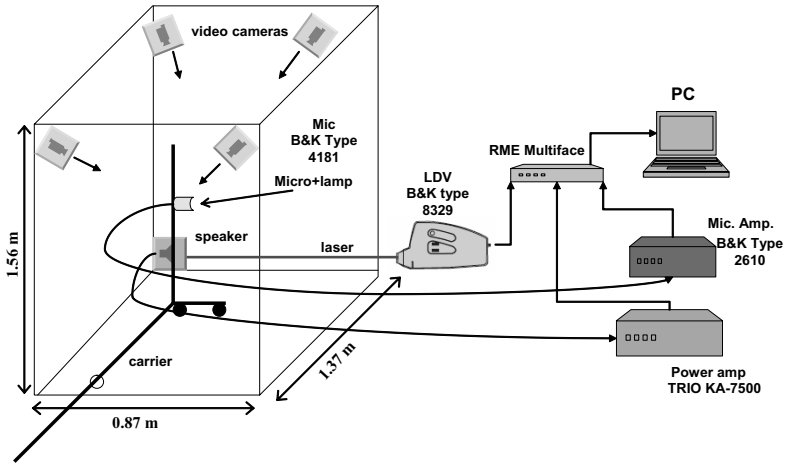

Figure 2: Artifacts used for the experiments.

The disposition of these surfaces is as follows: 1) two lateral walls covered with 50mm–32 Kg/m^3 glass wool (GW 50mm), 2) the floor covered with 5mm–96 Kg/m^3 wool felt (Felt 5mm), 3) a lateral window covered with 20mm–96 Kg/m^3 glass wool (GW 15mm), and 3) the rest bare walls and ceiling of the chamber (Rigid walls). The location of each surface is depicted in Figure 3b.

The parameters to be measured in the experiments are the vibration velocity of the sound source (speaker) and the complex sound pressures at M random points in the interior field. These parameters are expressed as

$$\begin{aligned} v_{\text{speaker}} &= |\mathrm{V}| \exp^{j(\omega t+\theta_{\text{speaker}})} \ , \\ p_f &= |\mathrm{P}| \exp^{j(\omega t+\theta_f)} \ . \end{aligned} \tag{13}$$

In steady-state the time factor is omitted and the phase reference can be chosen as the phase of the sound source. Thus, the vibration amplitude is directly measured with the Lased Doppler Vibrometer (LDV), and the phase and amplitude of the sound pressures are computed from the microphone and LDV signals. The position of the measurement points is acquired automatically with a set of video cameras installed in the interior to perform stereo tracking in real-time. Note that the automatic stereo tracking allows the microphone to be moved freely as the sound pressure is being acquired. However, the maximum displacement of the microphone $d_{\max}$ is determined by the analysis frequency f_s of the speaker tone, as prescribed by the Doppler relation formula:

$$d_{\max} = c \left(\frac{f_s + |\beta|}{f_s} - 1 \right) \ , \tag{14}$$

where c is the velocity of sound in the medium, and β is the tolerated frequency deviation (in Hz) of the signal observed at the microphone.

4 Experimental results

After measuring a set of sound pressure amplitude and phase at 1000 different points in the interior of the experimental chamber, the iterative algorithm is provided with this data and initialized with an starting guess $\mathbf{z}^{(0)} = \mathbf{1}$ (i.e. the relative impedance of the propagation media). Moreover, the sought impedances were assumed to be within the space $-10,000 < \mathbf{z} < 10,000$ (normalized impedance values are assumed hereafter unless otherwise is specified). The 3D meshed model of the chamber is composed by 1446 constant-triangular elements with a maximum edge size of 0.12 m.

For the inverse analysis, four different homogeneous surfaces were considered as specified before, and the acoustic impedance values found by the iterative process are shown in Figure 4. Note that these values minimize the error between the BEM-predicted and the actual measured sound fields as low as 1.6% for the experiment at 80 Hz, and as high as 5.6% for 120 Hz. This rates can be observe in Figure 5 where the convergence history of the iterative process is shown. Although the stoping threshold was assigned as $\alpha = 0.01$ for all the experiments, none achieved this value, thus the iterations have to be stopped before the process jumps to a solution space that fits the noise components of the input data. In the current implementation, a criterion of minimum improvement was used to stop the iterations.

In general, although the results seem to agree with what expected, let us point that, for the understanding of the authors, by the moment there is no other method reported in the literature that allows us to measure the acoustic impedance of the materials under experimental conditions similar to those presented here. Therefore, a validation method, together with a generally applicable stopping criterion, is currently under development.

5 Conclusions

In this paper, a method to estimate the normal-incidence acoustic impedance of the surfaces in interiors has been described. The method itself differs from traditional methods in which the estimation of acoustic impedances is formulated as an inverse boundary problem. Approaching the problem in this way is what allows the method to be used with complex-shape surfaces, making possible at the same time the estimation of the acoustic impedance of not only one but all the surfaces in the interior (provided that their geometry is known). Moreover, the system employs only one microphone to measure the sound pressure in the interior field, thus helping to overcome some other physical constraints that existent methods suffer. On the other hand, the fundamental requirement to achieve accurate estimations of the acoustic impedances is that the test surfaces should be locally reactive, or at least the local reaction effect should be predominant. This condition is usually found in empty rooms, therefore, the method introduced here is particularly useful to assess the boundary values when numerical analysis of such rooms are performed.

Although the development of this technique is in an experimental stage, the preliminary experiments performed in a controlled environment showed that the inverse approach presented here yields, indeed, an estimate of the acoustic impedance on the surfaces. Moreover, segmenting and grouping the surface according to their homogeneity leads to considerable improvement of the robustness to noise by reducing the degrees of freedom of the inverse problem. Feature that suggests the potential application of the method in real interiors.

Nevertheless to say that there are difficulties to overcome before experimenting in a real environment: the computational cost is huge since the current implementation is based on the boundary element method, thus requiring the computation and storage of two $N \times N$ matrices and two $M \times N$ matrices. Note, however, that the iterative algorithm proposed here requires only the evaluation of an objective function at each iteration. Therefore, more efficient boundary element frameworks (e.g. the Fast Multipole Boundary Element Method, [9]) that do not need to store dense matrices are currently under consideration for the future implementation of the algorithm.

References

[1] M. Garai, "Measurement of the sound absorption coefficient in situ, the reflection method using periodic pseudo random sequences of maximum length", *Applied Acoustics*, **39**, 119–139(1993).

[2] J. F. Allard, C. Depoiller and P. Guignouard, "Free field surface impedance measurements of sound absorbing materials with surface coatings", *Applied Acoustics*, **26**, 199–207(1989).

[3] A. J. Cramond and C. G. Don, "Reflection of impulses as a method of determining the acoustic impedance", *J. Acoust. Soc. of Am.*, **75**, 328–344(1984).

[4] E. Mommertz, "Angle-dependent in situ measurement of reflections coefficients using a substraction technique", *Applied Acoustics*, **46**, 251–264(1995).

[5] R. Lanoye, G. Vermeir and W. Lauriks, "Measuring the free field acoustic impedance and absorption of sound absorbing materials with a combined particle velocity-pressure sensor", *J. Acoust. Soc. of Am.*, **119**, 2826–2831(2006).

[6] Y. Takahashi, T. Otsuru and R. Tomiku, "In situ measurements of surface impedance and absorption coefficients of porous materials using two microphones and ambient noise", *Applied Acoustics*, **66**, 845–865(2005).

[7] J. D. Maynard, E. G. Williams and Y. Lee, "Nearfield Acoustic Holography: I. Theory of the generalized holography and the developement of the NAH", *J. Acoust. Soc. Am.*,**78**, 1395–1413(1985).

[8] G. Dutilleux, F. C. Sgarg and U. R. Kristiansen, "Low-frequency assessment of the in situ acoustic absorption of materials in rooms: an inverse problem approach using evolutionary optimization", *Int. J. Numer. Meth. Eng.*, **53**, 2143–2161(2002).

[9] T. Sakuma and Y. Yasuda, "Fast Multipole Boundary Element Method for large-scale steady-state sound field analysis. Part I: Setup and validation", *Acta Acustica united with Acustica*, **88**, 513–525(2002).

1: Using $\mathbf{z}^{(0)}$, solve for $\tilde{\mathbf{v}}_S^{(\ell)}$ from

$$(\mathbf{C}_S - \tilde{\mathbf{B}}_S)\tilde{\mathbf{v}}_S = \hat{\mathbf{B}}_S\hat{\mathbf{v}}_S \tag{9}$$

2: **while** condition (12) is **false do**

3: Update $\mathbf{z}$ by

$$\mathbf{z}^{(\ell+1)} = \arg\min \|\langle \mathbf{A}_f \cdot \tilde{\mathbf{v}}_S^{(\ell)} \rangle \, \mathbf{z} - \tilde{\mathbf{B}}_f \tilde{\mathbf{v}}_S^{(\ell)} - \hat{\mathbf{p}}_f\| \quad \text{s.t.} \quad \mathrm{Z}_{\min} \leq \mathbf{z} \leq \mathrm{Z}_{\max} \tag{10}$$

4: Update $\tilde{\mathbf{v}}_S^{(\ell+1)}$ using $\mathbf{z}^{(\ell+1)}$ in Eq. (9)

5: Compute $\mathbf{p}_g$ by

$$\mathbf{p}_g = \hat{\mathbf{B}}_f\hat{\mathbf{v}}_S - (\mathbf{C}_f - \tilde{\mathbf{B}}_f)\tilde{\mathbf{v}}_S^{(\ell+1)} \tag{11}$$

6: Evaluate

$$\frac{\|\mathbf{p}_g - \mathbf{p}_f\|^2}{\|\mathbf{p}_f\|^2} \leq \alpha \tag{12}$$

7: $\ell \leftarrow \ell + 1$

8: **end while**

Algorithm 1: Iterative estimation of $\mathbf{z}$

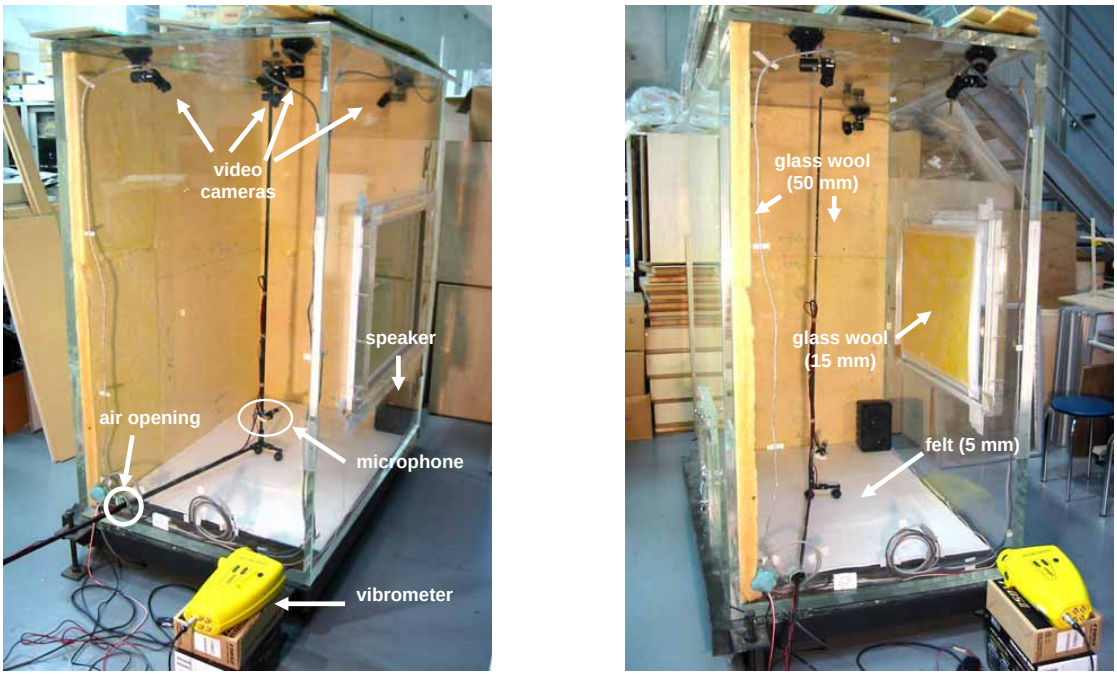

a) **b)**

Figure 3: a) The actual experimental setup. b) Materials and surfaces considered for the preliminary experiments.

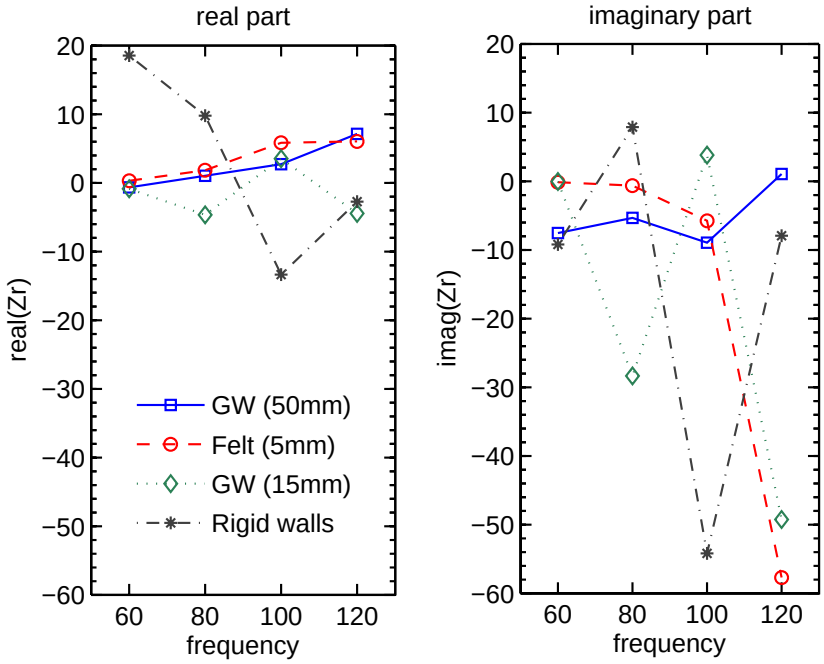

Figure 4: Complex acoustic impedance (normalized values) obtained from the experiments.

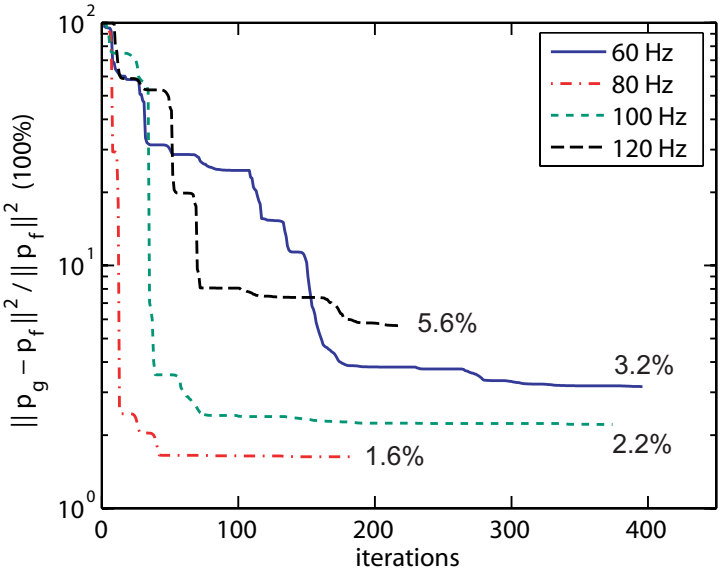

Figure 5: Convergence history of the iterations for the estimation of $\mathbf{z}$ with the experimental data.